Applied Catalysis B: Environmental 91 (2009) 563–572

Contents lists available at ScienceDirect

Applied Catalysis B: Environmental

journal homepage: www.elsevier.com/locate/apcatb

Electrochemical synthesis of novel structured catalysts for H_2 production

Francesco Basile [a], Patricia Benito [a], Giuseppe Fornasari [a], Valentina Rosetti [a], Erika Scavetta [b], Domenica Tonelli [b], Angelo Vaccari [a,*]

[a] Dipartimento Chimica Industriale e dei Materiali, ALMA MATER STUDIORUM-Università di Bologna, Viale Risorgimento 4, 40136 Bologna, Italy
[b] Dipartimento Chimica Fisica e Inorganica, ALMA MATER STUDIORUM-Università di Bologna, Viale Risorgimento 4, 40136 Bologna, Italy

ARTICLE INFO

Article history:
Received 13 March 2009
Received in revised form 23 June 2009
Accepted 27 June 2009
Available online 3 July 2009

Keywords:
H_2 production
Structured catalyst
Electrochemical synthesis
Hydrotalcite-type compound
Nickel
Metallic foam
Steam methane reforming

ABSTRACT

Innovative catalysts supported on metallic foams (FeCrAlloy) have been prepared by electrochemical synthesis of Ni-containing hydrotalcite-type (HT) films, and used in the steam methane reforming. It consisted of a one-step synthesis and deposition of HT compounds on metallic supports after the application of a cathodic potential on the foam. The effects of synthesis parameters, applied potential (−0.9 and −1.2 V) and time (600, 1000 and 1800 s), on the properties of the supported films and catalytic performances were investigated. The potential applied mainly affected the rate of the basic media generation in the vicinity of the electrode, which is responsible for the precipitation of the HT compounds. The pulse length was the key factor to determining both the coverage of the support and the thickness of the film. Moreover, the Ni- and Al-content in the catalyst depended on both factors. The synthesis conditions affected the steam reforming tests performed under industrial-type conditions. The selection of optimum synthesis conditions (−1.2 V for 1000 s) led to a well-adhered catalyst film, showing catalytic performances close to the thermodynamic equilibrium and stable with increasing time-on-stream. Furthermore, this preparation method offers the opportunity to develop processes with increasing chemico-energetic efficiency of endothermic reactions.

1. Introduction

H_2 is expected to become a major source of energy in the future. The reforming of hydrocarbons, especially steam methane reforming (SMR), is currently the most common and most economical way to obtain H_2 [1,2]. However, the steam reforming process is endothermic and high temperatures are required. Moreover, the active phase is mainly supported on oxide pellets (i.e. insulating materials), thus thermal conductivity is low, and thermal profile is steep, so even higher temperatures must be maintained outside the reactor tubes and high residence times are required to increase the temperature along the bed. Industrial reactors usually consist of a series of small-diameter metal tubes containing steam reforming pelletized catalysts surrounded by heaters [3]. In this configuration, the overall thermal efficiencies obtained approach 95%; however, just 50% of the heat produced by combustion in the burners is used directly for the steam reforming enthalpy. Furthermore, temperature gradients take place both longitudinally – from the inlet to the outlet of the tubes – and radially across the wall, creeps occur, and the lifetime of the tubes is reduced [4,5]. In short, although steam reforming is a mature technology, its main drawbacks have yet to be overcome to improve the overall process, for both large-scale production and microfuel applications [6].

Especially in small scale H_2 production, the development of novel catalysts in which the active phase is supported over a structured metallic support (foams, plates, reactor walls) is a promising alternative to conventional pelletized catalysts [7]. Although commonly applied in environmental technologies [8,9], they are an emerging field in H_2 production processes [10,11]. These catalysts offer advantages such as a decrease in pressure drop and high mechanical strength. Moreover, by selecting metallic materials as support, an enhanced heat transfer by conduction, which is not available for the random packing of catalyst pellets, is also achieved. In particular, metal foams having interconnected porous structure, and attractive thermal and mechanical properties, meet all the requirements of light weight, low pressure drop, easy shaping, improved gas mixing, and heat transfer. However, some drawbacks can be found during the deposition of catalysts on the metallic structure, which are related to the adhesion between support and catalyst, because of the low metallic–ceramic material interaction. Moreover, by taking into account the larger expansion coefficient of the metals as compared to that of ceramics, rupturing and cracks between the washcoat layer and the support must be avoided [12]. In short, the selection of the support and the preparation method are key points. Many

* Corresponding author. Tel.: +39 051 2093683; fax: +39 051 2093680.
E-mail address: angelo.vaccari@unibo.it (A. Vaccari).

0926-3373/$ – see front matter © 2009 Published by Elsevier B.V.
doi:10.1016/j.apcatb.2009.06.028

different metals and alloys have been proposed for the manufacture of supports [13]. Ferritic alloys, e.g. stainless steel containing a small amount of Al, such as FeCrAlloy foams, are interesting materials for high-temperature applications, such as the SMR, because of their excellent ability to resist oxidation and corrosion. After oxidation, a slow growing of an alumina layer protects the foam from corrosion and improves the anchoring of the catalytic coating [14]. Most methods reported in literature involve the pre-treatment of the support followed by deposition of a ready-made catalyst [15,16].

In a previous paper [17], the authors reported on a new method for the preparation of FeCrAlloy foams covered by hydrotalcite-type (HT) compounds, which are precursors of SMR catalysts. HTs are lamellar compounds of chemical formula $[M_{1-x}^{2+}M_x^{3+}(OH)_2][A^{b-}]_{x/b}\cdot nH_2O$ [18]. A wide variety of compounds can be prepared by modifying both the nature of the layers and the interlayer region in order to obtain materials with specific properties. Compounds containing nickel and noble metals are precursors of active catalysts in natural gas conversion processes, such as catalytic partial oxidation, steam and dry reforming [19]. After calcination and reduction, metallic particles are obtained, which are well dispersed, highly active, and stabilized against sintering, coke formation, and oxidation. Although HT compounds are commonly synthesized by co-precipitation, new synthetic routes have been developed over the last few years to obtain solids with improved properties. Among all of these, electrochemical deposition was used to prepare modified electrodes [20–23]. It consisted of applying a cathodic potential in a three-electrode cell containing a nitrate solution of the metallic salts leading to the generation of OH^-. Because of the basic media, the hydrotalcite precipitates close to and on the surface of the working electrode (platinum) [20,24]. Since FeCrAlloy foams are electrically conductive, a similar synthesis procedure for preparing catalysts active in the SMR process was adopted, where the working electrode was a FeCrAlloy foam. Unlike conventional deposition methods involving two-step processes, this new method consists of the one-step electrosynthesis of Ni,Al–NO_3 HT phase on the surface of the foam in a very short time [17]. Furthermore, other advantages are that simple and inexpensive equipment is required, films can be obtained on large and irregular surfaces, the deposition occurs closer to equilibrium than with high-temperature methods, and inter-element diffusion is not a problem; lastly, the process can be controlled because of its electrical nature.

Previously [17], we reported that both the potential applied and the synthesis time strongly affect catalytic performances. Here, a more detailed explanation about this method is provided in terms of the characterization of deposited HT precursors and calcined products for establishing a structure–catalytic activity relationship. The paper deals with the tests of structured catalysts in the SMR reaction under industrial-type conditions, nevertheless both the technique and the catalytic materials, thanks to the versatility of the HT precursors, can be used in other processes involving large enthalpy change (endo- or exothermic processes).

2. Experimental

2.1. Catalyst preparation

The Ni/Al–NO_3 HT film was deposited on metallic FeCrAlloy foams, by cathodic reduction of a 0.03 M solution containing $Ni(NO_3)_2\cdot 6H_2O$, $Al(NO_3)_3\cdot 9H_2O$ (molar ratio 3/1) and 0.3 M KNO_3. Electrosynthesis in the same conditions was also carried out on FeCrAlloy plates, to allow a complete characterization of the deposited material. Electrochemical synthesis was carried out at room temperature (r.t.) by using a single-compartment, three-electrode cell. Electrode potentials were measured with respect to an aqueous saturated calomel electrode (SCE; i.e. reference electrode [R.E.]). A Pt wire was used as the counter electrode (C.E.). The working electrode (W.E.) was the conductive material to be covered with HT phase, i.e. the FeCrAlloy foam. The electric contact was established by inserting a platinum wire inside the foam. FeCrAlloy foams (80 ppi) were obtained by cutting cylinders of 12 mm diameter and 10 mm long from a panel; in the middle of the foam a channel was cut out to host the thermocouple shell (average bare foam weight 0.2700 g). Chronoamperometric (CA) curves were recorded using a CH instrument Mod. 660C controlled by a personal computer running CH Instrument software. Electrosynthesis was carried out at two different deposition times and potentials (Table 1); after electrosynthesis, the films were gently rinsed with doubly distilled water and dried. Catalysts were prepared by calcinating the deposited foams at 900 °C for 12 h and they were labeled by adding the prefix "ex" to the name, e.g. exHT-0.9-600.

Table 1
Samples prepared by electrosynthesis.

Sample	Applied potential (V) *vs* SCE	Time (s)	Solid deposited (wt.%)
HT-0.9-600	−0.9	600	nd
HT-0.9-1800	−0.9	1800	1.2
HT-1.2-600	−1.2	600	1.5
HT-1.2-1000	−1.2	1000	2.2

Reference catalysts were prepared by a conventional washcoating method of a Ni,Al–CO_3 HT phase with Ni/Al = 3/1. The foam was pretreated at 900 °C for 12 h, washcoated with a disperal solution (10 wt.% in H_2O with 0.4% HNO_3), and finally washcoated with a dispersion of the HT compound in water (20 wt%); the procedure was repeated twice.

2.2. Catalytic activity

Catalytic tests were carried out in an Incoloy 800HT reactor, with 9 mm thick walls and 12 mm inner diameter, placed inside an electric oven. Six foam cylinders were loaded in the isothermal zone of the reactor for 6 cm in height, while filling the bottom and top section of the tube with inert materials (beads of corundum or quartz pellets). A thermocouple wire was inserted along the axial direction of the reactor, into which a chromel–aluminum thermocouple can be slid to measure the axial thermal profile during reaction. SMR tests were carried out at: P = 20 bar, S/C = 1.7, T_{oven} = 900 °C and CT = 4 s. Contact time was calculated by using the total gross volume of the foam substrate (6 ml) at r.t., regardless of cell density, catalyst loading and washcoat concentration [10]. The feed was provided by a cylinder of pure CH_4 and a HPLC pump for water. Water was vaporized using a heater at 400 °C and then mixed with methane before entering the reactor. Catalysts were activated by in situ reduction at 900 °C for 2 h with a H_2/N_2 equimolar flow. During start-up, steam was firstly fed to avoid carbon deposition, while in the shut-down the steam was switched off after the methane.

Wet syngas passed through a water condenser to separate the major amount of non-reacted water. Dry syngas was then analyzed on line by using a two gas-chromatograph equipped with HWD: a Fisons Instruments 8000 Series and a Perkin Elmer AutoSystem XL, equipped with Carbosieve S-II 100–120 mesh-packed columns: N_2 and He were used, respectively, as carrier gas in the analysis of H_2 and other products (CO, CO_2, and CH_4).

2.3. Characterization techniques

X-ray diffraction (XRD) patterns were collected with Cu Kα radiation (λ = 1.5418 Å) by means of a X'PertPro PANalytical diffractometer equipped with a fast X'Celerator detector. The 3–

80° 2θ range was measured performing steps of 0.07° (2θ) and counting 120 s/step. The analyses were performed on a powder that was gently removed from a FeCrAlloy plate with the aid of a lancet. A "zero background" sample holder (The Gem Dugout, State College, PA, USA) was used. FT-IR spectra were recorded by using a Perkin-Elmer 1750 instrument. The analyses were carried out on the powder, scratched from the FeCrAlloy plate, using KBr pellets; 16 spectra (recorded with a nominal resolution of 4 cm^{-1}) were averaged to improve the signal-to-noise ratio. Thermogravimetric (TG) analyses were carried out in a TGA 2050 instrument from TA instruments in flowing air, at a heating rate of 10 °C min^{-1} from 30 to 1000 °C. Temperature programmed reduction and oxidation (TPR/O) analyses were carried out with an H_2/Ar and an O_2/N_2 5/95 (v/v) gas mixture respectively (total flow rate 20 ml/min) in the 60–950 °C temperature range in a ThermoQuest CE Instruments TPDRO 1100. Supported metallic foams were used directly as specimens for measurements. SEM/EDS analyses were performed by using an EVO 50 Series Instrument (LEO ZEISS) equipped with an INCAEnergy 350 EDS micro-analysis system and INCASmart-Map for imaging the spatial variation of elements in a sample (Oxford Instruments Analytical). The accelerating voltage was 25 kV, the beam current 1.5 nA, and the spectra collection time 100 s. Element chemical analysis was carried out by ICP-AES in a Fisons 3410 instrument. The adhesion of the electrosynthesised catalyst layer was studied by submitting coated foams to ultrasounds in an ultrasonic bath Bandelin SONOREX SUPER RK510 working at 35 kHz. Coated foams were immersed in petroleum ether inside a sealed beaker and submitted to ultrasounds for 10 and 40 min at r.t., then the samples were dried at 40 °C. During the electrochemical synthesis, local pH near the foam was measured with acid–base indicators (all purchased from Sigma–Aldrich). The pH range from 6.0 to 12.0 was covered: Bromothymol blue (from yellow to blue in the pH range 6.0–7.6), Cresol red (from yellow to red in the pH range 7.2–8.8), Phenolphthalein (from colorless to pink in the pH range 8.2–9.6), Thymolphthalein (from colorless to blue in the pH range 9.3–10.5), Yellow Alizarin GG (from yellow to purple in the pH range 10.5–12.0). A 0.01 wt.% aqueous solution of a selected indicator was used in every experiment. Two drops of a selected indicator were added to a colorless KNO_3 solution whose pH was adjusted to 3.3 with HNO_3 in order to simulate the pH of the deposition solution. The potential step was applied to observe the change in the color of the indicator.

3. Results and discussion

3.1. Catalytic activity

Supported catalysts were tested in the steam methane reforming (SMR) process under industrial-type conditions (S/C = 1.7, P = 20 bar, CT = 4 s and T_{oven} = 900 °C) (Fig. 1). Differences in SMR activity and syngas selectivity were observed on the basis of synthesis conditions (potential applied and time) [17]. The catalyst obtained at −0.9 V for 600 s, exHT-0.9-600, showed a poor SMR activity. Methane conversion was rather low and it steadily decreased with the increase of the time-on-stream. Moreover, the selectivity in CO_2 and the H_2/CO ratio gradually increased (while CO and H_2 selectivity decreased) due to the water gas shift reaction (WGSR). Despite the steam excess (S/C = 1.7), the decreased conversion of methane led to a higher partial pressure of steam, so the WGSR promoted the CO_2 formation. By increasing the deposition time, from 600 to 1800 s, exHT-0.9-1800, after an initial

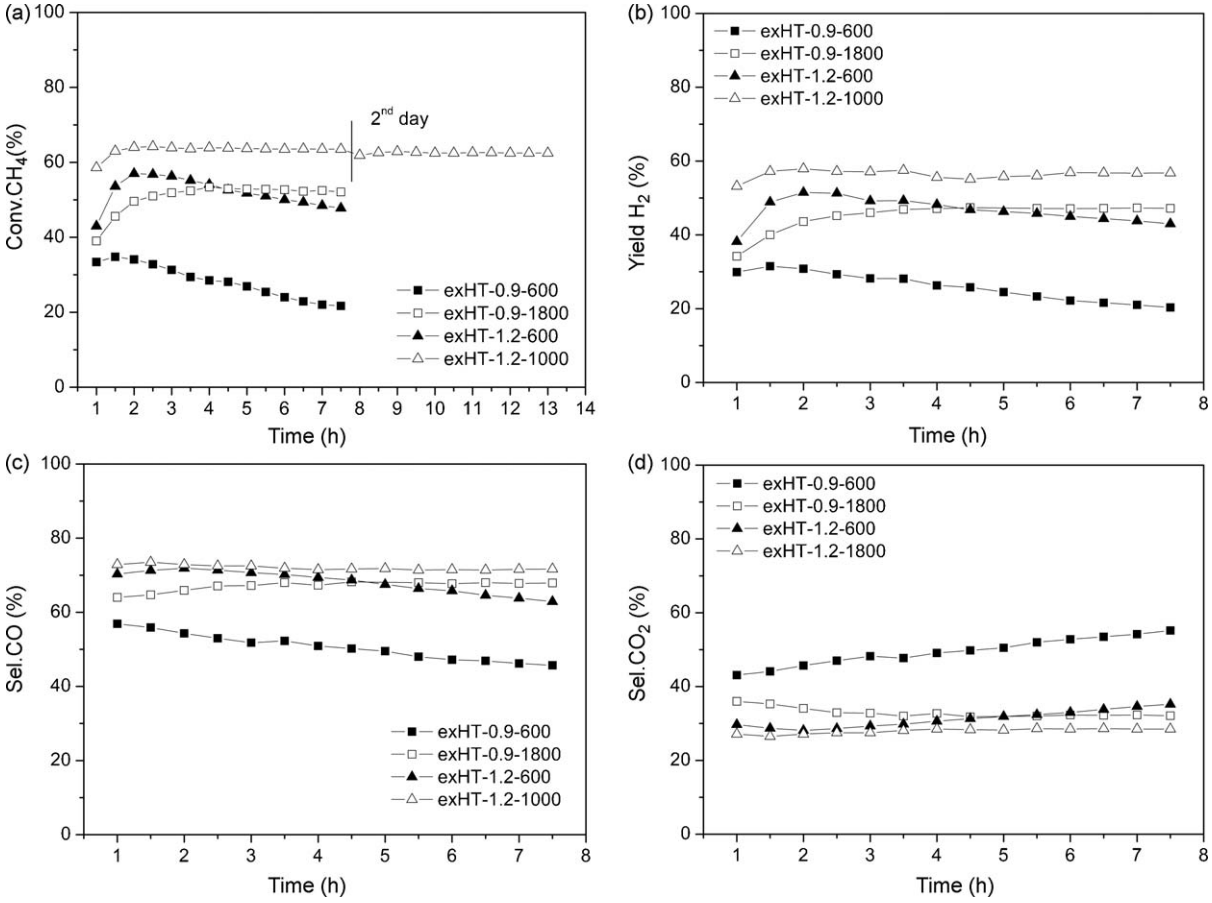

Fig. 1. CH_4 conversion (a), H_2 yield (b), CO (c) and CO_2 (d) selectivity of the samples prepared by electrochemical synthesis under different conditions.

activation step during the first hour, the steady-state condition was reached. Methane conversion and selectivity in syngas increased when compared to exHT-0.9-600, probably due to an increase in the Ni-content and film stability; however, values were still far from the thermodynamic equilibrium.

The change in the applied potential, −1.2 V instead of −0.9 V, also led to an improvement in the initial catalytic performance, but deactivation was observed when synthesis was performed for 600 s, exHT-1.2-600. Conversely, by prolonging synthesis time for 1000 s, exHT-1.2-1000 catalyst, after a steady increase in catalytic activity during the first hour, the activity neared the equilibrium value (64% instead of 67% equilibrium). Two-day tests were performed to study its stability. An activation period was observed due to both the reduction of partially oxidized Ni^0 to Ni^{2+} by steam during shut-down and start-up operations [25] and the low number of Ni active sites. Once the reaction started, the reducing atmosphere led to a slight activation and catalytic performances were constant, indicating that the coating was relatively stable under severe reaction conditions.

Considering the type of structured catalyst and the change in the synthesis conditions, the two main parameters affecting the catalytic activity and stability may be Ni-content and film homogeneity; therefore characterization was carried out in order to determine the effect of each of them.

3.2. Characterization

3.2.1. HT precursors

The surface morphology and chemical composition of HT electrosynthesised materials was studied by SEM and EDS analyses, respectively. For comparison purposes the bare foam was also characterized. The bare metallic foam showed pores with a mean size of about 200–300 μm. After electrodeposition, regardless of the synthesis conditions, blockage of the pores was not observed (Fig. 2). However, both the amount of solid deposited (see Table 1) and the film morphology strongly depended on potential and time (Fig. 3). Performing syntheses at −0.9 V, HT-0.9-600 and HT-0.9-1800 samples (Fig. 3a and b), the support was covered by a thin film and small aggregates of particles grew over it. This feature may be related to a different mechanism of solid growth once the electrode is fully covered if compared to when the metallic surface was completely exposed [26]. The coating was not homogeneous: the deposition first took place on the most exposed areas (Fig. 4), because exposed and irregular surfaces are more conducive to deposition (which must be considered just a mechanical process) [27]. The same behavior was observed when syntheses were performed at −1.2 V (Fig. 3c and d). However, in this case, extending the synthesis time up to 1000 s, HT-1.2-1000, particles uniformly covered the surface of the support. Small, uniform platelets of HT were deposited on the surface, forming a sponge-type structure. For comparison purposes, a Ni,Al HT compound was deposited by the conventional washcoating method. SEM images showed that some foam pores were blocked and the coverage was not uniform. A detailed comparison of the electrochemical versus conventional method will be reported elsewhere [28]. The advantage of using electrochemical synthesis was the fast and homogeneous pH increase in the vicinity of the foam, leading to the precipitation of small, uniformly sized particles on the surface foam [23]. It is well known that the adhesion of the coat depends on the particle size of the deposited powders; this takes place primarily by a mechanical mechanism and, to a much lesser extent, via a chemical or affinity mechanism; thus the deposition of small particles would increase the adhesion on the substrate [27].

The compositional analysis of the as-deposited film was carried out by EDS analysis; in particular, the Ni/Al molar ratio was evaluated, giving useful information on the formation of pure HTs or the presence of side-phases [28]. The results obtained are summarized in Table 2. Firstly, it should be taken into account that because of the thin supported film, the chemical information given by the EDS analysis included Al from both the support and the solid; therefore, the former was subtracted in the results reported in Table 2. Moreover, since a non-planar surface could be studied, the reported results only gave a semi-quantitative information about the composition of the layer. The composition of the HT-0.9-600 sample was not uniform all over the surface; an Al-rich solid with a very low Ni/Al ratio (<0.1 and 0.6) was obtained. Prolonging the synthesis time (1800 s) led to the incorporation of further Ni^{2+} cations, but Ni/Al values were still far from those in the original solution (3/1). Likewise, the chemical composition was not homogeneous: a Ni/Al ratio of 1.0 was obtained in flat zones, whereas on the tips (where there was a larger amount of electrosynthesised solid) a 2.0 Ni/Al ratio was measured. On the other hand, samples prepared at −1.2 V, HT-1.2-600 and HT-1.2-1000, showed a uniform chemical composition and Ni/Al ratios were 2.1 and 3.4, respectively. Taking into account the fact that pure HT compounds can be obtained in the 2–4 Ni/Al interval [29], it could be assumed that at −0.9 V an Al-rich phase was probably obtained as a non-desired phase whereas, by increasing the potential applied, the Ni/Al ratio was in the range of the formation of pure HT compounds.

In order to confirm the formation mechanism, ICP analyses were performed on the powder deposited on FeCrAlloy plates at −0.9 V for 1800 s and at −1.2 V for 1000 s and scratched away. The Ni/Al ratio for the sample HT-0.9-1800 was 0.64, while for the sample HT-1.2-1000 a 2.8 value was determined. The results

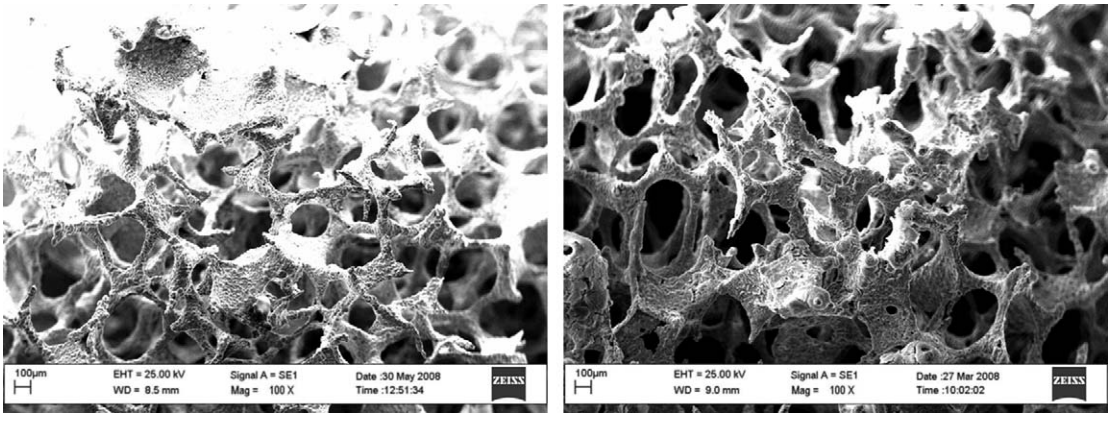

Fig. 2. SEM images of the samples prepared at longer synthesis time: HT-0.9-1800 (left) and HT-1.2-1000 (right).

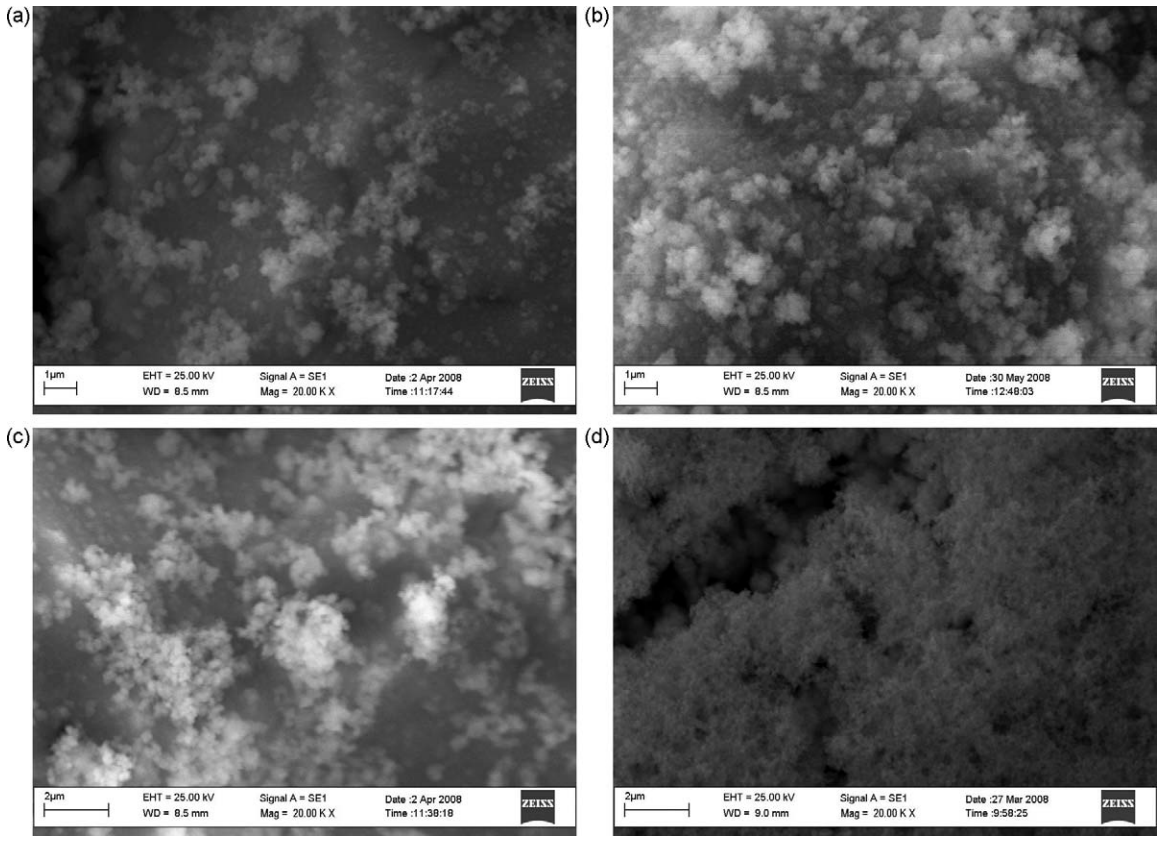

Fig. 3. Detailed SEM images of the foams with HT phases obtained under different synthetic conditions ((a) HT-0.9-600; (b) HT-0.9-1800; (c) HT-1.2-600; (d) HT-1.2-1000).

confirmed those obtained by EDS: at −0.9 V an Al-rich solid was obtained, whereas increasing the potential, the Ni-amount in the solid increased. However, it should be considered that the use of a plate instead of a foam as the working electrode, slightly modified the features of the electrochemical cell (geometry, conductivity of the electrode surface, way of assuring the electrical contact) and therefore the rate of the nitrate reduction as well as the pH may be different than those with the foam. Finally, several analyses (PXRD, FT-IR and TG) were performed on a sample prepared at −1.2 V for 1000 s on a FeCrAlloy plate to confirm the formation of the HT phase.

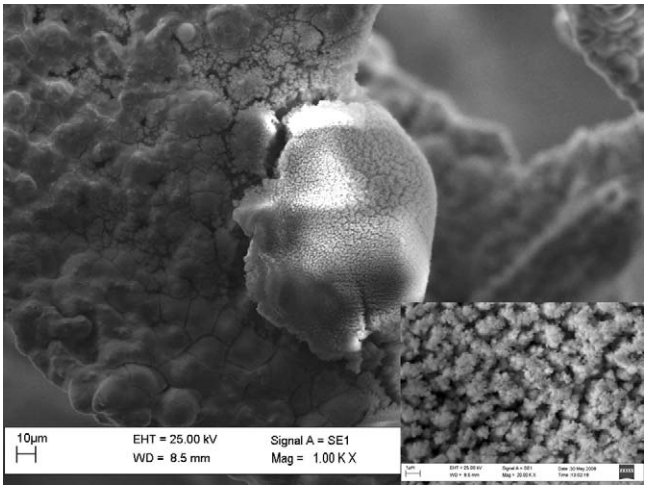

Fig. 4. Detailed SEM images of the preferential deposition on the most exposed areas at different magnifications (sample HT-0.9-1800). Inset: high magnification image.

The diffraction pattern of the HT-1.2-1000 sample (Fig. 5) confirmed the formation of the HT structure during electrosynthesis [29]. The broad and not well-defined diffraction lines, however, indicated that a poorly crystallized solid was obtained. The basal spacing (8.01 Å) corresponded to a HT compound with nitrate anions intercalated between hydroxyl sheets adopting a "flat-lying" configuration, with the molecular plane of nitrate parallel to the hydroxyl layers [30]. The "flat-lying" arrangement was also in agreement with the high Ni/Al ratio obtained by EDS; however, the presence of carbonate anions with high affinity in the interlayer space could cause a significant reduction in basal spacing.

FT-IR spectrum (Fig. 6) was also characteristic of HT compounds with nitrate anions in the interlayer region [31]. The broad band at about 3470 cm^{-1} was related to the stretching vibration mode, ν_{OH}, of hydroxyl groups from the layers and from water molecules both physisorbed and intercalated. The bending mode of water molecules, δ(HOH), was observed at around 1640 cm^{-1}. The presence of nitrate anions was confirmed by the sharp and intense band at 1384 cm^{-1} due to the ν_3 (E') vibrational mode. The small peak at about 1025 cm^{-1} due to the ν_1 mode of nitrates, an inactive IR mode, pointed to a decreased symmetry of the anion from D_{3h} to C_{2v}, which is probably related to the low crystallinity of the solids in which no symmetric interactions between layer and interlayer

Table 2
Ni/Al ratio calculated from EDS analyses of the supported HTlcs (Zone 1: flat zone; Zone 2: tip of the foam).

Sample	Zone 1	Zone 2
exHT-0.9-600	<0.1	0.6
exHT-0.9-1800	1.0	2.0
exHT-1.2-600	2.1	2.2
exHT-1.2-1000	3.2	3.4

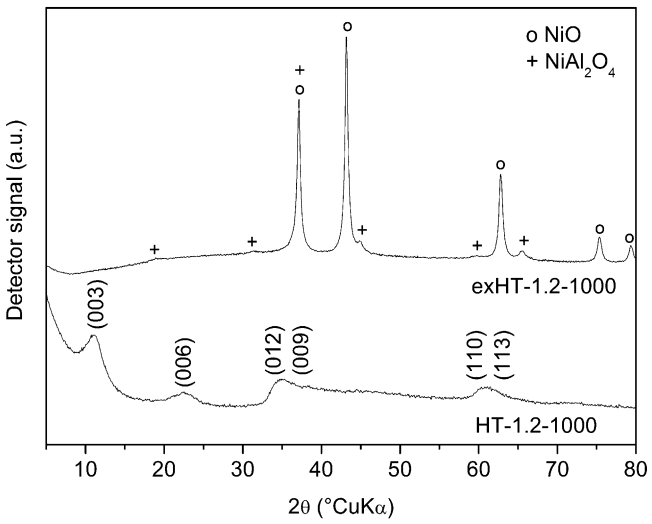

Fig. 5. PXRD pattern of the solid obtained at −1.2 V for 1000 s in a FeCrAlloy plate as prepared and after calcination at 900 °C for 12 h.

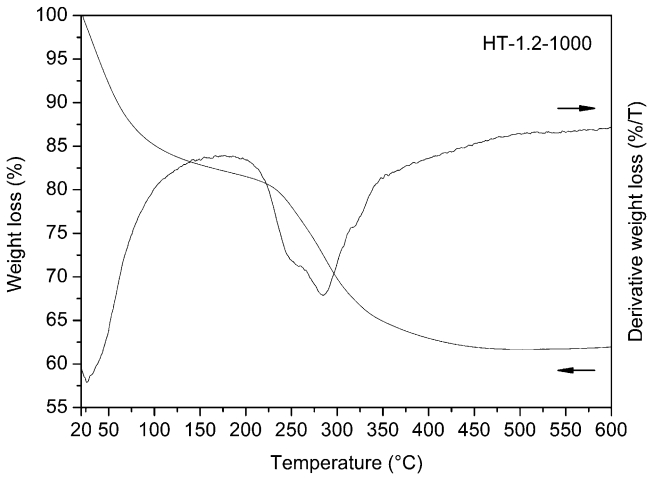

Fig. 7. TG and DTG profiles recorded in air of the sample obtained at −1.2 V for 1000 s on a FeCrAlloy plate recorded in air.

were established. Moreover, the broad band lying below the nitrate band in the 1500–1200 cm^{-1} range was attributed to contaminant carbonate species. The ν_2 and ν_4 modes of both nitrate and carbonate species were recorded in the low wavenumber region, together with vibrational modes of hydroxide sheets, thus making the assignment rather difficult [31].

The thermogravimetric curve of HT-1.2-1000 is shown in Fig. 7 in which only the 30–600 °C range has been reported, since no weight loss was detected in the further range up to 1000 °C. A two-step decomposition was observed, with a total weight loss of 35%, in agreement with previous results for Ni,Al compounds [32]. The low decomposition temperatures were related to the high Ni/Al ratio, because HT compounds with a low Al^{3+} content showed a poorer thermal stability [33]. The first step was due to the removal of physisorbed and interlamellar water. The second step extended up to 400 °C. This thermal decomposition included several processes: the removal of hydroxyl groups from layers as water; the removal of interlayer water molecules; the decomposition of carbonates, as CO_2, and nitrates, evolved as NO_2. A careful inspection indicated that it consisted of two overlapped weight losses, ascribed to the dehydroxylation and posterior depletion of NO_3^- anions as reported by Xu and Zeng [33] for samples with low aluminum content.

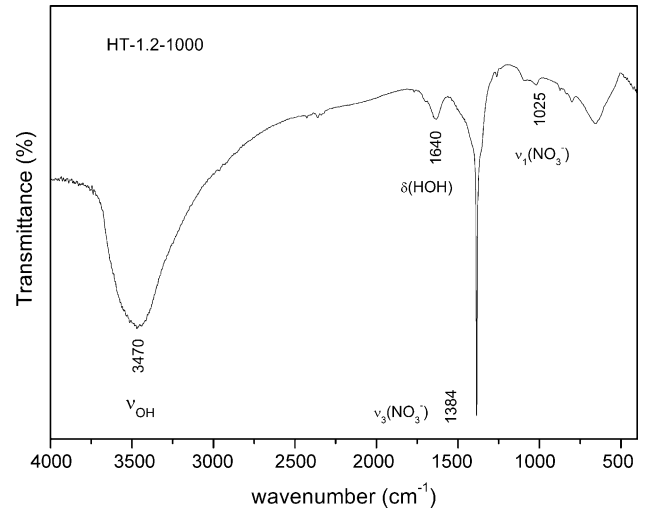

Fig. 6. FT-IR spectra of the sample obtained at −1.2 V for 1000 s in a FeCrAlloy plate.

In conclusion, it could be stated that the HT structure was obtained by electrochemical synthesis over FeCrAlloy. In order to establish the mechanism of the HT phase formation, the pH in the vicinity of the electrode was measured. Unfortunately, despite several attempts, it was not possible to observe the color change of the indicator when it was added to a solution containing nickel and aluminum salts. Thus, measurements were performed in a 0.3 M KNO_3 solution, with an initial pH similar to that in the metal solution in order to mimic actual synthesis conditions. Furthermore, it must be kept in mind that during potentiostatic synthesis, the cell current might decrease, because of both the low diffusion rates of reactant molecules [24] and the change in conductivity of the metallic foam as the solid film grows. In this situation, the nitrate reduction rate and, therefore, the base generation could be altered. Consequently, the procedure reported here gave the pH at the beginning of the synthesis. Stable pH values were reached at about 50 s; i.e. by prolonging the pulse time the pH did not increase, but the generation of the basic media was extended throughout the bulk of the solution. At −0.9 V the pH in the vicinity of the foam was low, between 6.5 and 7.5, thus supporting the low Ni/Al ratio of the solids obtained by EDS and ICP. Conversely, when the potential was increased (−1.2 V) the reduction of nitrates, which led to the basic media, took place faster and to a greater extent; higher pH values (8.7–9.6) were obtained, being in the range of a Ni-based HT phase precipitation. Therefore, it could be stated that whereas the potential applied during the electrosynthesis was the main parameter for determining the pH close to the electrode, responsible for precipitation (and therefore its chemical composition), the synthesis time was the parameter controlling both the thickness and the film composition. In order to explain the slow incorporation of Ni^{2+} species, it should be considered that this reaction was described as diffusion-limited [34], and since syntheses were performed at r.t. the mass transfer was very low.

Taking into account the above-mentioned results, it could be stated that the mechanism of HT phase formation on the surface of the foam at low potential (−0.9 V) took place through a two-step mechanism. In the early period, the local increase of pH led to precipitation of mainly acidic Al^{3+} cations, as hydroxide or oxyhydroxide phases. Then, the pH increased, leading to the co-precipitation of Ni^{2+} and Al^{3+} cations as a HT compound. The process was completed by the re-dissolution and re-precipitation of the Al-hydroxides previously precipitated. This mechanism agreed with previously reported results for the synthesis of Mg,Al HT compounds by homogeneous precipitation using urea as the

precipitation agent [35,36], where the basic medium was generated by an in situ reaction as in electrochemical synthesis. At a higher potential, −1.2 V, the rate of basic media generation was much faster, reaching a higher pH value. Under these conditions, the Al^{3+} precipitation as hydroxide may occur just in the very early stages of the synthesis, while the co-precipitation mechanism was predominant. Results were in line with a previous work [23], where the authors observed that when the electrochemical synthesis was performed over platinum electrodes and the salt concentration solution was 0.03 M (similar to that used in these experiments), the pure Ni,Al HT phase was always observed, even at low synthesis times. In the present work, replacing the working Pt electrode with FeCrAlloy, because of the lower conductivity of the latter a higher potential (−1.2 instead of −0.9 V) was required to obtain predominant co-precipitation. In fact, at low potential, the poor conductivity of the foam decreased the rate of nitrate reduction and, therefore the OH^- formation with respect to the OH^- consumption (hydroxide precipitation); consequently, the isolation of the individual steps was observed.

3.2.2. Catalysts

Calcination at high temperatures (900 °C) of Ni/Al–NO_3 HT compounds yielded to NiO and $NiAl_2O_4$ phases (Fig. 5). After calcination at 900 °C, the $NiAl_2O_4$ spinel segregated and the excess of nickel formed the NiO phase [28], thus the NiO/$NiAl_2O_4$ ratio depended on the Ni/Al ratio in the precursor: the highest was the Ni-content in the precursor, and most NiO phase formed in the final catalyst. TPR/O gave some evidence of the chemical composition in terms of the identification of Ni-containing species with different reducibility. For comparison, the TPR of the bare foam was measured and no H_2 consumption was observed. TPR profiles of exHT-1.2-600 and exHT-1.2-1000 samples are shown in Fig. 8. Two main H_2 consumption peaks were observed for both samples, the one at lower temperature (434 and 456 °C respectively for the samples prepared for 600 and 1000 s) was attributed to the reduction of bulk NiO weakly interacting with the support, while the peak at higher temperature, around 900 °C, corresponded to the reduction of $NiAl_2O_4$, in spite of the fact that at least two other shoulders are present at temperatures close to 570 and 820 °C. The ratio between the areas of NiO/$NiAl_2O_4$ reduction peaks was in line with the Ni/Al ratio in the precursor. This means that a smaller NiO peak was recorded for the exHT-1.2-600 sample due to the lower Ni-content. Furthermore, it should be noted that the characterization of the calcined bare foam revealed the segregation of Al-containing species from the foam forming Al_2O_3 during thermal treatment [37]. Thus, the solid state reaction between some Ni^{2+} in the deposited solid and the alumina segregated from the foam could be significant, especially at the low coverage conditions [38], affecting the NiO/$NiAl_2O_4$ ratio.

As previously reported in the catalyst section, during the shut-down and start-up of the reformer plant the oxidation of Ni^0 particles occurred because of the exposure to steam, whereas once the reaction started Ni-containing species reduced again. During the oxidation-reduction process, some structural changes may occur in the catalyst. In order to obtain more information about the behavior of the catalyst, after the reduction in the TPR instrument, the sample was submitted to another oxidation–reduction cycle. Almost similar TPR profiles of fresh and oxidized catalysts were obtained, thus indicating that although the Ni^{2+} cations are reduced and extracted from the bulk of the supported structure, after oxidation they formed NiO phase or reacted with the alumina to form the $NiAl_2O_4$ phase again. The difference in the reduction temperature of the first peak became significant between exHT-1.2-600 and exHT-1.2-1000 catalysts indicating the presence of free NiO or a NiO sintering. The reduction of $NiAl_2O_4$ was shifted to a lower temperature and the doublet peak of the exHT-1.2-1000

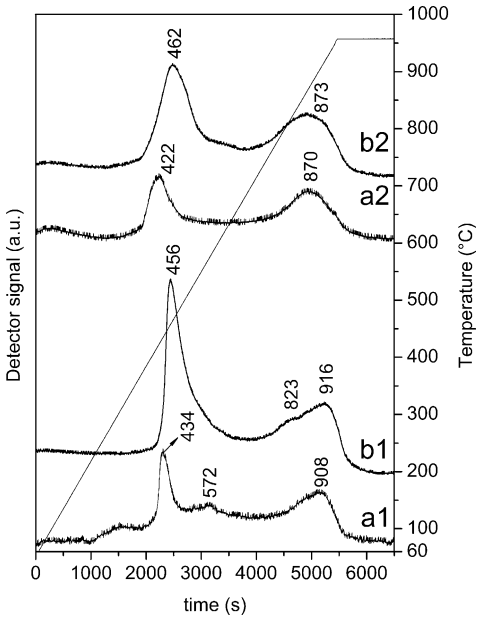

Fig. 8. TPR profiles of exHT-1.2-600 ((a1) 1st reduction and (a2) 2nd reduction) and exHT-1.2-1000 ((b1) 1st reduction and (b2) 2nd reduction).

sample was reduced to one, due to the interaction of NiO with the Al_2O_3 matrix forming a homogeneous $NiAl_2O_4$ phase. The ratio of the NiO/$NiAlO_4$ peak decreased due to an increase in the Ni-amount present as spinel.

As expected, the morphology of supported catalysts after calcination at 900 °C was also strongly related to the synthesis conditions (Fig. 9). Firstly, it should be pointed that HT compound decomposition was accompanied by a weight loss of around 35% as shown by TG analysis, with a consequent shrinking of the particles, so it was quite difficult to avoid the formation of voids on the surface of the films. The characterization of supported catalysts prepared at low potential, −0.9 V (Fig. 9a and b), revealed that they mainly consisted of a homogenous Al-rich thin layer (both coming from the support and from the solid deposited) formed by small particles, where the nickel produced by exHT compounds was dispersed. On the other hand, SEM images of exHT-1.2-600 catalyst (Fig. 9c) showed that the solid film was not homogeneously distributed over the foam, and isolated areas with diameter between 10 and 50 μm covered by catalyst were observed. When increasing the electrosynthesis time, exHT-1.2-1000 catalyst (Fig. 9d), the deposited solid film was retained after the thermal treatment and, moreover, it seemed to be more compact and with an improved adherence.

The adherence of the catalyst layer to the metallic foam was studied by submitting the samples to ultrasounds for increasing times from 10 to 40 min. It was not possible to evaluate the weight loss due to the catalyst layer detachment, since the amount of solid deposited was very low. Instead, SEM was used to evaluate the stability of the film after 40 min of ultrasonication (see Supplementary information, Fig. S1). The film was partially detached in catalysts obtained from the precursors prepared at shorter times at both potentials. Whereas, the morphology of the catalyst layer remained almost unmodified for exHT-0.9-1800 and exHT-1.2-1000 catalysts (i.e. for longer times).

The morphology of the coating after catalytic tests was evaluated by SEM/EDS (Figs. 10 and 11). Unloaded exHT-0.9-600 catalyst was constituted by alumina needles (Fig. 10a), as in the fresh sample, small Ni^0 particles were deposited on it; however, some uncovered zones were observed due to the detachment of the catalyst during the tests. Furthermore, amorphous and filamentous

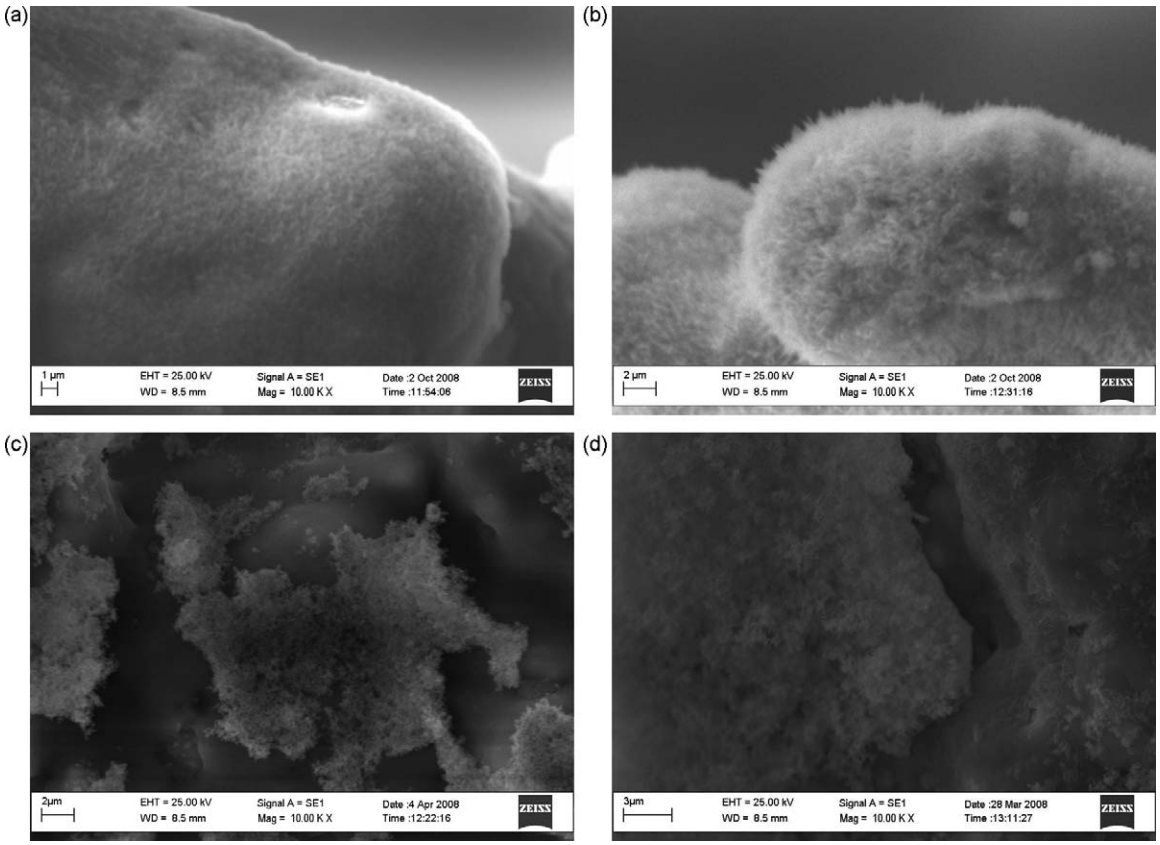

Fig. 9. SEM images of the catalysts obtained by calcination at 900 °C for 12 h ((a) exHT-0.9-600; (b) exHT-0.9-1800; (c) exHT-1.2-600; (d) exHT-1.2-1000).

carbon were observed, which accumulated in the pores of the foam (Fig. 10b). In exHT-0.9-1800 catalyst the coating was constituted by a homogeneous layer of alumina whiskers, wherein Ni^0 particles were highly dispersed (Fig. 10c). Large alumina particles were also observed (Fig. 10d), which seemed to form from the aggregation of the whiskers. On the other hand, in some zones, together with the alumina whiskers, Ni^0 particles highly interacting with the support were also observed. The morphology of the catalysts prepared at −1.2 V after the catalytic tests was different from those obtained at −0.9 V. The surface of the exHT-1.2-600 was not homogeneous, and three main regions were observed: (i) some uncoated struts due to the detach of the layer during the catalytic tests; (ii) some "islands" of catalyst with Ni^0 particles supported on them (Fig. 11a); (iii), uniformly sized Ni^0 particles on an alumina phase (Fig. 11b), corresponding to the zones where a larger amount of catalyst has been deposited. Finally, in the unloaded exHT-1.2-1000 catalyst, Ni^0 particles were supported on a homogeneous alumina layer (Fig. 11c) or large alumina grains (Fig. 11d).

3.3. Discussion of the catalytic results

To summarize, if we take into account the characterization results of fresh and unloaded catalysts, the performances of electrosynthesised catalysts may be explained considering the Ni-amount in the catalyst layer, the stability and the homogeneous distribution of the supported film. When syntheses were performed at −0.9 V, the poor SMR activity and stability of the catalyst prepared for 600 s, was related to the low amount of Ni-containing species and to the low stability of the film coating the support together with the carbon formation. On the other hand, the catalytic performances of exHT-0.9-1000 catalyst were stable with increasing time-on-stream due to the stability of coating and the high dispersion of the Ni-containing particles; however, the Ni-amount was not sufficient to achieve acceptable methane conversion values. On the other hand, when the potential applied was −1.2 V, the Ni-content was greater and both catalysts showed enhanced catalytic performances during the first hour. However, the catalyst prepared by a shorter time, exHT-1.2-600, deactivated because the presence of coating faults. If this catalyst is compared with the more homogeneous exHT-0.9-1800 catalyst, even if the Ni-loading is lower the overall activity became higher after few hour of time-on-stream. Conversely, catalytic performances obtained with exHT-1.2-1000 catalyst were close to the thermodynamic equilibrium, due to a higher content of active species and the stability of the thin layer of catalyst, which is formed by small particles with an improved adhesion to the substrate.

As shown in our previous communication [17], this catalyst showed an activity similar to that of a commercial catalyst (average CH_4 conversion 64% instead of 59.6% for the commercial sample), despite the remarkably lower content (gNi^{2+}(commercial) = 0.885 and gNi^{2+}(exHT-1.2-1000) = 0.012). The lower catalyst loading was compensated by both the improved thermal transfer of the metallic support and the enhanced effectiveness factor for deposited particles, due to the high geometric area of the metallic foam, thus leading to a better utilization of the catalyst [39]. Furthermore, for electrosynthesised samples, the thin catalyst film, around 1 μm, further increased the efficiency factor: nickel was almost fully utilized, as it was observed in the SEM images of the unloaded catalyst, the Ni^0 particles were available to the reactant gas, in contrast with conventional washcoated catalysts prepared by repetitive coatings, where active sites of inner layers could be covered with those of outer layers, thus leading to a constant decrease in available active sites [40]. In addition, during the thermal process, the migration of alumina to the surface may take place, although this film did not produce the cracking and

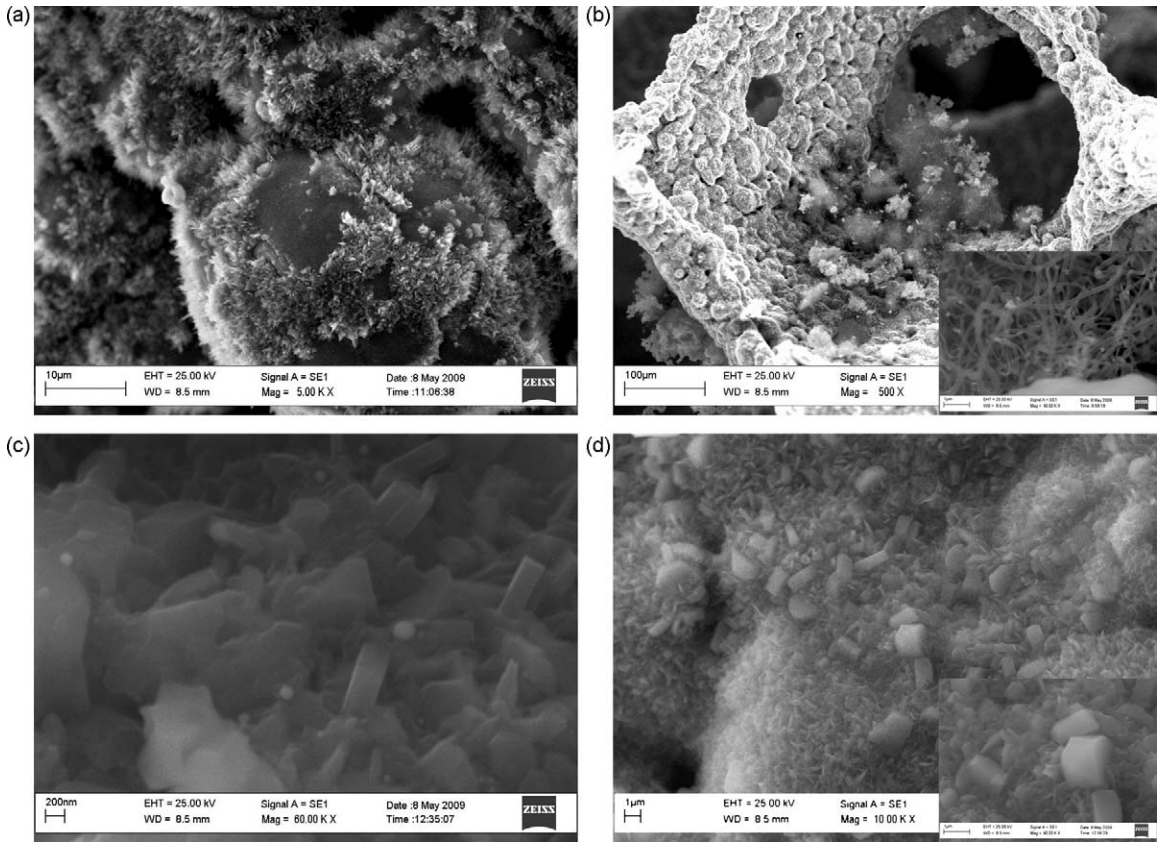

Fig. 10. SEM images of exHT-0.9-600 (a and b) and exHT-0.9-1800 (c and d) catalysts after the catalytic tests. Inset: high magnification images.

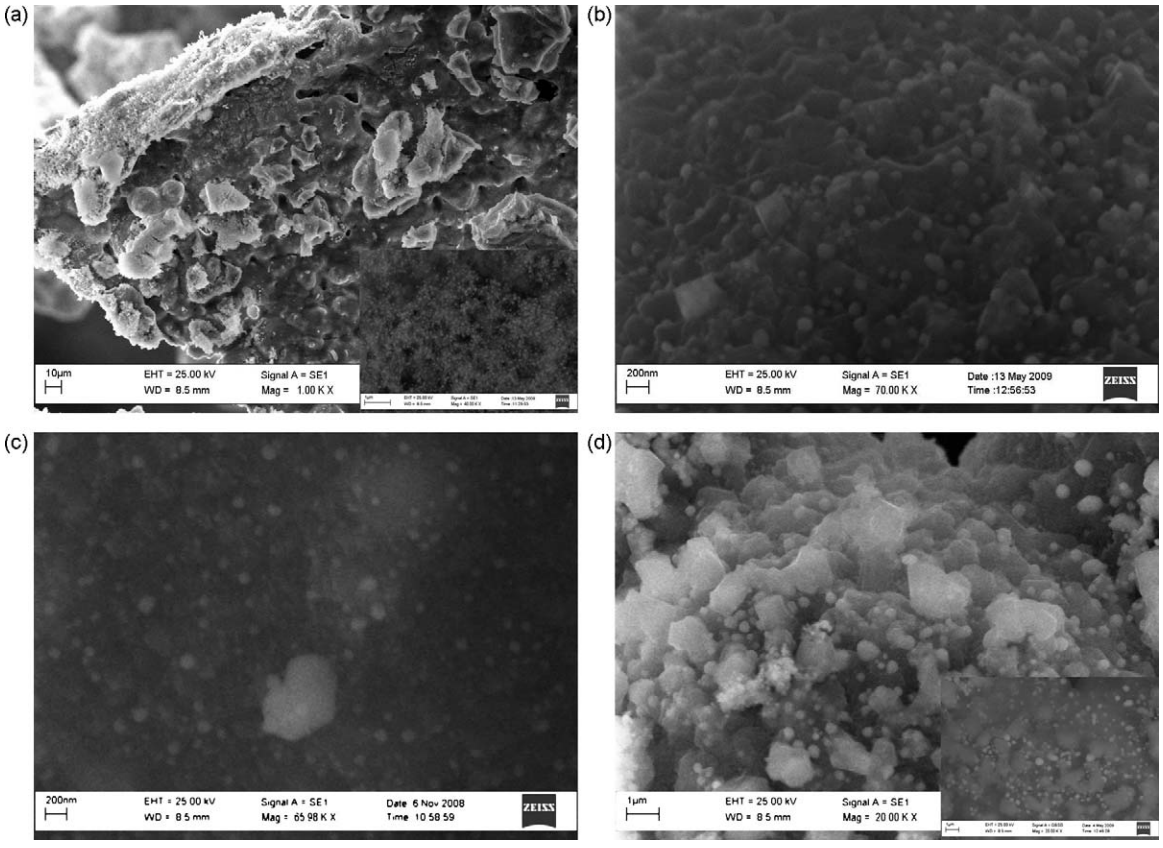

Fig. 11. SEM images of exHT-1.2-600 (a and b, inset: high magnification) and exHT-1.2-1000 (c and d, inset: backscatter electron image) catalysts after the catalytic tests.

release of the surface film. The formation of interfacial compounds could play a key role in the bonding of the catalyst to the metallic substrate, thus improving its adhesion and, therefore, its stability. Lastly, it should be noted that previous results indicated that hydrothermal conditions used in SMR create several material changes (corrosive degradation of the metal, delamination of the washcoated catalyst from the metal support, and accelerated sintering) by interfering with the performances of the catalyst [41]. Instead, by choosing the electrochemical synthesis it was possible to use FeCrAlloy as the support for Ni-based catalysts, avoiding the above mentioned drawbacks.

4. Conclusions

The synthesis of Ni,Al HT films over FeCrAlloy foams, which are precursors of SMR catalysts, was performed using a novel and simple electrochemical method. The HT films were successfully prepared with the metallic foam replacing the working electrode in a three-electrode cell, in which the basic medium was generated by the reduction of nitrates. The film characteristics may be controlled and modified by changing the synthesis conditions, in particular the applied potential (−0.9 and −1.2 V), and the synthesis time (600, 1000, and 1800 s). The potential applied mainly affected the pH in the vicinity of the foam, while the deposition time determined the film thickness. Performing the electrosynthesis at −0.9 V, since the pH in the vicinity of the foam was low, an Al-rich compound precipitated on the support. The Ni incorporation increased prolonging the synthesis from 600 to 1800 s. After thermal treatment a homogeneous and well-distributed film was obtained, which is responsible for the stable methane conversion obtained with the catalyst prepared for 1800 s, in spite of the low Ni-content. On the other hand, when the applied potential was −1.2 V, a suitable pH for the HT compound formation was achieved faster. The highest Ni-contents led to an improved methane conversion and syngas selectivity at the beginning of the catalytic tests. However, the morphology of the deposited film played an important role in the stability of the catalyst. The poorly distributed solid film after calcination in the sample prepared for 600 s generated a catalyst deactivation by increasing time-on-stream. The catalyst obtained at 1000 s showed stable performances, which approached thermodynamic equilibrium, despite the low Ni-content. The thin and well-adhered film enhanced the density of active sites per unit mass (or volume), thus improving the efficiency of the catalyst material. Finally, it is noteworthy that the present method is a powerful preparation tool for the preparation of films on structured supports and reactors for the H_2 production by reforming and could be extended and applied in a series of highly endothermic and exothermic reactions.

Acknowledgements

The authors acknowledge to Prof. M. Gazzano for his help in the XRD measurements. The financial support from MIUR (Rome)-PRIN program is gratefully acknowledged.

Appendix A. Supplementary data

Supplementary data associated with this article can be found, in the online version, at doi:10.1016/j.apcatb.2009.06.028.

References

[1] J.N. Armor, Appl. Catal. A 176 (1999) 159.
[2] J.R. Rostrup-Nielsen, J. Sehested, J. Nørskov, Adv. Catal. 47 (2002) 65.
[3] D.E. Ridler, M.V. Twigg, in: M.V. Twigg (Ed.), Catalyst Handbook, 2nd ed., Wolfe Publishing, London, 1989.
[4] J.R. Rostrup-Nielsen, Catal. Today 106 (2005) 293.
[5] S. Gevskott, T. Rusten, M. Hillestad, E. Edwin, O. Olsvik, Chem. Eng. Sci. 56 (2001) 597.
[6] P. Ferreira-Aparicio, M.J. Benito, J.L. Sanz, Catal. Rev. 47 (2005) 491.
[7] A. Cybulski, J.A. Moulijn (Eds.), Structured Catalysts and Reactors, CRC Taylor & Francis, Boca Raton, 2005.
[8] R.M. Heck, R.J. Farrauto (Eds.), Catalytic Air Pollution Control: Commercial Technology, Wiley, New York, 1995.
[9] P. Avila, M. Montes, E. Miró, Chem. Eng. J. 109 (2005) 11.
[10] T. Giroux, S. Hwang, Y. Liu, W. Ruettinger, L. Shore, Appl. Catal. B 56 (2005) 95.
[11] R.J. Farrauto, Y. Liu, W. Ruettinger, O. Ilinich, L. Shore, T. Giroux, Catal. Rev. 49 (2007) 141.
[12] R.M. Heck, S. Gulati, R.J. Farrauto, Chem. Eng. J. 82 (2001) 149.
[13] M.V. Twigg, D.E. Webster, in: A. Cybulski, J.A. Moulijn (Eds.), Structured Catalysts and Reactors, CRC Taylor & Francis, Boca Raton, 2005, pp. 71–108.
[14] X. Wu, D. Weng, S. Zhao, W. Chen, Surf. Coat. Technol. 190 (2005) 434.
[15] T.A. Nijhuis, A.E.W. Beers, T. Vergunst, I. Hoek, F. Kapteijn, J.A. Moulijn, Catal. Rev. 43 (2001) 345.
[16] V. Meille, Appl. Catal. A 315 (2006) 1.
[17] F. Basile, P. Benito, P. Del Gallo, G. Fornasari, D. Gary, V. Rosetti, E. Scavetta, D. Tonelli, A. Vaccari, Chem. Commun. (2008) 2917.
[18] X. Duan, D.G. Evans, in: D.M.P. Mingos (Ed.), Layered Double Hydroxides, Structure and Bonding, vol. 119, 2006.
[19] S. Albertazzi, F. Basile, A. Vaccari, in: F. Wypych (Ed.), Clay Surfaces: Fundamentals and Applications, Elsevier, Amsterdam, 2004, p. 496.
[20] E. Scavetta, B. Ballarin, M. Giorgetti, I. Carpani, F. Cogo, D. Tonelli, J. New Mater. Electrochem. Syst. 7 (2004) 43.
[21] B. Ballarin, M. Berrettoni, I. Carpani, E. Scavetta, D. Tonelli, Anal. Chim. Acta 538 (2005) 219.
[22] E. Scavetta, B. Ballarin, M. Berrettoni, I. Carpani, M. Giorgetti, D. Tonelli, Electrochim. Acta 51 (2006) 2129.
[23] E. Scavetta, A. Mignani, D. Prandstraller, D. Tonelli, Chem. Mater. 19 (2007) 4523.
[24] G.H.A. Therese, P.V. Kamath, Chem. Mater. 12 (2000) 1195.
[25] T. Ohi, T. Miyata, D. Li, T. Shishido, T. Kawabata, T. Sano, K. Takehira, Appl. Catal. A 308 (2006) 194.
[26] T. Mahalingam, S. Velumani, M. Raja, S. Thanikaikarasan, J.P. Chu, S.F. Wang, Y.D. Kim, Mater. Charact. 58 (2007) 817.
[27] C. Agrafiotis, A. Tsetsekou, A. Ekonomakou, J. Mater. Sci. Lett. 18 (1999) 1421.
[28] F. Basile, P. Benito, S. Bugani, W. De Nolf, G. Fornasari, K. Janssens, L. Morselli, E. Scavetta, D. Tonelli, A. Vaccari, submitted for publication.
[29] F. Cavani, F. Trifirò, A. Vaccari, Catal. Today 11 (1991) 173.
[30] Z.P. Xu, H.C. Zeng, J. Phys. Chem. B 105 (2001) 1743.
[31] J.T. Kloprogge, D. Wharton, L. Hickey, R.L. Frost, Am. Miner. 87 (2002) 623.
[32] D. Tichit, F. Medina, B. Coq, R. Dutartre, Appl. Catal. A 159 (1997) 241.
[33] Z.P. Xu, H.C. Zeng, Chem. Mater. 13 (2001) 4564.
[34] J.W. Boclair, P.S. Braterman, Chem. Mater. 11 (1999) 298.
[35] M. Adachi-Pagano, C. Forano, J.-P. Besse, J. Mater. Chem. 13 (2003) 1988.
[36] P. Benito, F.M. Labajos, V. Rives, Cryst. Growth Des. 6 (2006) 1961.
[37] L. Giani, C. Cristiani, G. Groppi, E. Tronconi, Appl. Catal. B 62 (2006) 121.
[38] S.H. Zeng, Y. Liu, Appl. Surf. Sci. 254 (2008) 4879.
[39] J.-H. Ryu, K.-Y. Lee, H. Lab, H.-J. Kim, J.-Il Yang, H. Jung, J. Power Sources 171 (2007) 499.
[40] X. Du, D. Gao, Z. Yuan, N. Liu, C. Zhang, S. Wang, Int. J. Hydrogen Energy 33 (2008) 3710.
[41] B.R. Johnson, N.L. Canfield, D.N. Tran, R.A. Dagle, X.S. Li, J.D. Holladay, Y. Wang, Catal. Today 120 (2007) 54.